An 11.5 W Yb:YAG planar waveguide laser fabricated via pulsed laser deposition

James A. Grant-Jacob,* Stephen J. Beecher, Tina L. Parsonage, Ping Hua, Jacob I. Mackenzie, David P. Shepherd, and Robert W. Eason

Optoelectronics Research Centre, University of Southampton, Highfield, Southampton SO17 1BJ, UK
**jagj1v11@soton.ac.uk*

Abstract: We present details of the homo-epitaxial growth of Yb:YAG onto a <100> oriented YAG substrate by pulsed laser deposition. Material characterization and initial laser experiments are also reported, including the demonstration of laser action from the 15 μm-thick planar waveguide generating 11.5 W of output power with a slope efficiency of 48%. This work indicates that under appropriate conditions, high-quality single-crystal Yb:YAG growth via pulsed laser deposition is achievable with characteristics comparable to those obtained via conventional crystal growth techniques.

OCIS codes: (120.4610) Optical fabrication; (130.0130) Integrated optics; (140.3380) Laser materials; (230.7390) Waveguides, planar; (310.0310) Thin films; (310.1860) Deposition and fabrication.

References and links

1. J. I. Mackenzie, "Dielectric solid-state planar waveguide lasers: A review," IEEE J. Sel. Top. Quantum Electron. **13**(3), 626–637 (2007).
2. S. J. Beecher, T. L. Parsonage, J. I. Mackenzie, K. A. Sloyan, J. A. Grant-Jacob, and R. W. Eason, "Diode-end-pumped 1.2 W Yb:Y_2O_3 planar waveguide laser," Opt. Express **22**(18), 22056–22061 (2014).
3. D. P. Shepherd, S. J. Hettrick, C. Li, J. I. Mackenzie, R. J. Beach, S. C. Mitchell, and H. E. Meissner, "High-power planar dielectric waveguide lasers," J. Phys. D Appl. Phys. **34**(16), 2420–2432 (2001).
4. H. Baker, J. Lee, and D. Hall, "Self-imaging and high-beam-quality operation in multi-mode planar waveguide optical amplifiers," Opt. Express **10**(6), 297–302 (2002).
5. M. J. F. Digonnet and C. J. Gaeta, "Theoretical analysis of optical fiber laser amplifiers and oscillators," Appl. Opt. **24**(3), 333–342 (1985).
6. J. I. Mackenzie, J. W. Szela, S. J. Beecher, T. L. Parsonage, R. W. Eason, and D. P. Shepherd, "Crystal Planar Waveguides, a Power Scaling Architecture for Low-Gain Transitions," IEEE J. Sel. Top. Quantum Electron. **21**(1), 380–389 (2015).
7. C. Grivas, T. C. May-Smith, D. P. Shepherd, and R. W. Eason, "Laser operation of a low loss (0.1 dB/cm) Nd:$Gd_3Ga_5O_{12}$ thick (40 μm) planar waveguide grown by pulsed laser deposition," Opt. Commun. **229**(1-6), 355–361 (2004).
8. T. C. May-Smith, J. Wang, J. I. Mackenzie, D. P. Shepherd, and R. W. Eason, "Diode-pumped garnet crystal waveguide structures fabricated by pulsed laser deposition," 2006 Conf. Lasers Electro-Optics 2006 Quantum Electron. Laser Sci. Conf. (2006).
9. S. H. Waeselmann, S. Heinrich, C. Kraenkel, and G. Huber, "Lasing in Nd^{3+}-doped Sapphire," in *Advanced Solid State Lasers*, OSA Technical Digest (online) (Optical Society of America, 2015), p. ATu1A.6.
10. J. Lancok, M. Jelinek, and F. Flory, "Optical properties of PLD-created Nd:YAG and Nd:YAP planar waveguide thin films," in (1999), Vol. 3571, pp. 364–367.
11. M. Jelinek, J. Oswalda, V. Studnikaa, J. Lancok, M. Paveka, D. Chvostova, V. Slechtováa, K. Nejezchlebb, and A. Mackovác, "Optical properties of Er : YAG and Er : YAP materials and layers grown by laser," **5036**, 268–274 (2003).
12. M. Ezaki, M. Obara, H. Kumagai, and K. Toyoda, "Characterization of Nd:$Y_3Al_5O_{12}$ thin films grown on various substrates by pulsed laser deposition," Appl. Phys. Lett. **69**(20), 2977 (1996).
13. T. Shimoda, Y. Ishida, K. Adachi, and M. Obara, "Fabrication of highly ytterbium (Yb^{3+})-doped YAG thin film by pulsed laser deposition," Opt. Commun. **194**(1-3), 175–179 (2001).
14. T. C. May-Smith, A. C. Muir, M. S. B. Darby, and R. W. Eason, "Design and performance of a ZnSe tetra-prism for homogeneous substrate heating using a CO_2 laser for pulsed laser deposition experiments," Appl. Opt. **47**(11), 1767–1780 (2008).

#253375 Received 9 Nov 2015; accepted 30 Nov 2015; published 10 Dec 2015

15. T. C. May-Smith, C. Grivas, D. P. Shepherd, R. W. Eason, and M. J. F. Healy, "Thick film growth of high optical quality low loss (0.1dBcm^{-1}) Nd:$Gd_3Ga_5O_{12}$ on $Y_3Al_5O_{12}$ by pulsed laser deposition," Appl. Surf. Sci. **223**(4), 361–371 (2004).
16. "Inorganic Crystal Structure Database (ICSD)," http://icsd.cds.rsc.org.
17. K. A. Sloyan, "Multi-beam pulsed laser deposition for engineered crystal films," PhD Thesis, University of Southampton (2012).
18. F. D. Patel, E. C. Honea, J. Speth, S. A. Payne, R. Hutcheson, and R. Equall, "Laser demonstration of $Yb_3Al_5O_{12}$ (YbAG) and materials properties of highly doped Yb:YAG," IEEE J. Quantum Electron. **37**(1), 135–144 (2001).
19. B. Aull and H. Jenssen, "Vibronic interactions in Nd:YAG resulting in nonreciprocity of absorption and stimulated emission cross sections," IEEE J. Quantum Electron. **18**(5), 925–930 (1982).
20. S. A. Payne, L. L. Chase, L. K. Smith, W. L. Kway, and W. F. Krupke, "Infrared cross-section measurements for crystals doped with Er^{3+}, Tm^{3+}, and Ho^{3+}," IEEE J. Quantum Electron. **28**(11), 2619–2630 (1992).
21. W. F. Krupke, "Ytterbium solid-state lasers - the first decade," IEEE J. Sel. Top. Quantum Electron. **6**(6), 1287–1296 (2000).

1. Introduction

Planar waveguide lasers are small yet power-scalable devices, which, owing to their high surface area to volume ratio, have excellent thermomechanical properties [1–3]. They also have the advantage of allowing confinement of the pump and laser modes [4], significantly lowering laser thresholds in comparison to bulk lasers, provided propagation losses remain modest [5]. A planar waveguide laser, with appropriate control over the oscillating spatial mode, can thus be used as an efficient device to increase brightness over a wide range of wavelengths [6], though due to difficulties in their fabrication, practical implementation has been limited.

Pulsed Laser Deposition (PLD) is a growth technique that is both simple and versatile, combining the ability to deposit tailored films with deposition rates as high as ~10 μm per hour, which allows for the growth of films sufficiently thick for diode-pumped planar waveguide lasers within moderate time scales [7]. In PLD, a laser pulse incident on the surface of a target material produces a plasma plume, which, when incident on the surface of a single-crystal substrate maintained at an appropriate temperature, can enable single-crystal layers to be grown [2,8]. In PLD, crystal growth occurs far from equilibrium, which offers the potential for fabrication of materials and structures that are difficult or impossible to grow via conventional techniques from the melt, in thermal equilibrium or via Czochralski growth. This novel capability is exemplified by the recent report of growth of single-crystal Nd:Al_2O_3 and the first laser demonstration from this material [9].

Target materials for PLD can be single-crystal or poly-crystalline sintered ceramics, the latter allowing almost any desired composition to be used for deposition. However, owing to the desirability of epitaxial growth, the lattice mismatch between the deposited layer and the substrate should be as small as possible, as should the mismatch in their respective thermal expansion coefficients, to avoid strain between the two layers following post-growth cooling to ambient temperature. The rate of deposition can be controlled via the ablation laser fluence, wavelength, spot size, and repetition rate, in addition to the background gas composition and pressure in the chamber. PLD has previously been proven as a technique to grow doped YAG films for use as waveguides [10–13]. In this work, we have shown that this technique can be used to grow relatively thick films, e.g. a 15 μm-thick Yb:YAG crystal, and via control of stoichiometry, we have increased the refractive index of the deposited material with respect to the undoped substrate, creating a waveguide with a sufficiently high numerical aperture (NA) to allow pumping with a diode-bar laser. These key improvements have enabled us to produce what we believe to be the first PLD-grown laser producing greater than 10 W of output power. In this paper, we document the fabrication, material characterization and laser performance of the planar waveguide.

#253375 Received 9 Nov 2015; accepted 30 Nov 2015; published 10 Dec 2015

2. Crystal growth

Our experimental set-up for pulsed laser deposition is shown in Fig. 1. A 248 nm KrF, 20 ns pulse duration, excimer laser operating at a repetition rate of 20 Hz was focussed into a stainless steel vacuum chamber to produce a fluence of approximately 1.6 J cm^{-2} at the target surface. The target was a 1.4 at.% Yb-doped-YAG pressed ceramic disc, 5-mm thick and 50 mm in diameter. Using a pressed ceramic source material rather than single-crystal targets reduces the ablation threshold, due to a decrease in the penetration depth of the UV radiation into the target. The target was rotated via an offset cam assembly using a DC motor to increase its utilization by allowing ablation of a ring of approximately 10 mm in width near the outer edge of the target.

The substrate onto which the target material was deposited was a single-side polished <100> YAG substrate, 10 mm × 10 mm × 1 mm in size, with one larger face polished for epitaxial growth. A CO_2 laser (10.6 μm wavelength, maximum output power of 30 W), with its beam homogenized by a ZnSe tetraprism [14], was used to heat the substrate from its unpolished rear side. This method provides uniform substrate heating without causing the entire chamber to heat up, which would otherwise increase desorption of contaminants from the chamber walls [15]. Using this CO_2 laser, the substrate was heated to a temperature of ~900 °C before deposition. Ceramic alumina posts were used to support the substrate with minimum heat-sinking to ensure negligible temperature gradients across the substrate. The chamber was pumped down to a pressure of 4×10^{-4} mbar and then back-filled with oxygen to a pressure of 2×10^{-2} mbar before deposition to enable compensation for any oxygen deficiency in the as-grown film. Following deposition and subsequent cooling, opposing end-facets of the sample were lapped and polished plane parallel, resulting in a waveguide length of 8 mm.

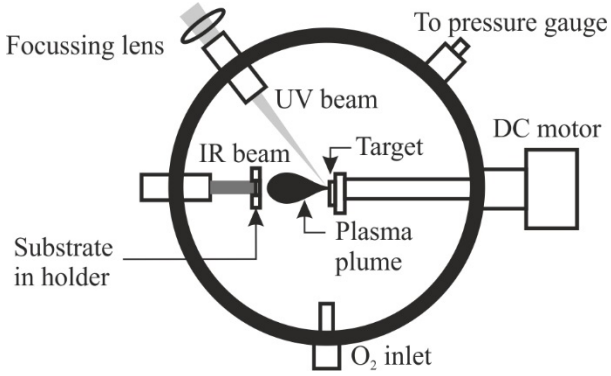

Fig. 1. Schematic of pulsed laser deposition set-up.

3. Material characterization

3.1. X-ray diffraction analysis

The deposited film had a thickness of 15 μm after a 4-hour growth run. X-ray diffraction (XRD) analysis was performed on this thin layer of Yb(1.4%):YAG using a Bruker D2 Phaser X-ray diffractometer that had a Cu K_α source (λ = 1.5406 Å) operating at 40 kV, while in-plane pole figure measurements of the sample were carried out using a Rigaku Smartlab X-ray diffractometer. The XRD spectrum displayed in Fig. 2(a), shows the presence of (400) and (800) peaks only, which indicates good epitaxial growth. A scan around the (400) peak is displayed in Fig. 2(b), showing that there is a slight shift in the (400) YAG peak to 29.60°, compared with the the expected database value for YAG at 29.76° [16] (an XRD spectrum from a blank YAG substrate is shown in red in Fig. 2(b), with highest peak normalized to highest green peak for ease of viewing). This is attributed to an aluminium deficiency in the

#253375 Received 9 Nov 2015; accepted 30 Nov 2015; published 10 Dec 2015

grown film caused by imperfect stoichiometric transfer of material from the target to the substrate during deposition. The secondary peaks of the Fig. 2(b), for the thin film and substrate, at 29.68° and 29.83° respectively, are due to secondary X-rays ($K_{\alpha 2}$) emitted from the source. The narrow FWHM of the (400) YAG 2θ peak of 0.1° and the lack of additional peaks at positions other than those from (400) and (800) YAG also indicates the material is predominately single crystal and follows the orientation of the substrate. The broad signal from 29.30 to 29.50° is likely a result of a region of lower quality crystal growth over an interfacial region that experienced a lower than ideal growth temperature.

Calibration of the shift in the diffraction peak, compared to the bulk YAG substrate, was determined through a combination of energy dispersive X-ray spectroscopy using a scanning electron microscope (SEM) and XRD measurements on additional bulk and PLD grown YAG samples, confirming a calculated deficiency in aluminium content of 2.5%. This non-stoichiometric transfer can occur in PLD due to preferential scattering of lighter elements by the background gas present in the chamber [17]. Hence, fine control of the aluminium to yttrium ratio can be achieved by careful control of deposition parameters, e.g. background gas pressure, substrate temperature, laser fluence, or increasing the aluminium concentration in the target.

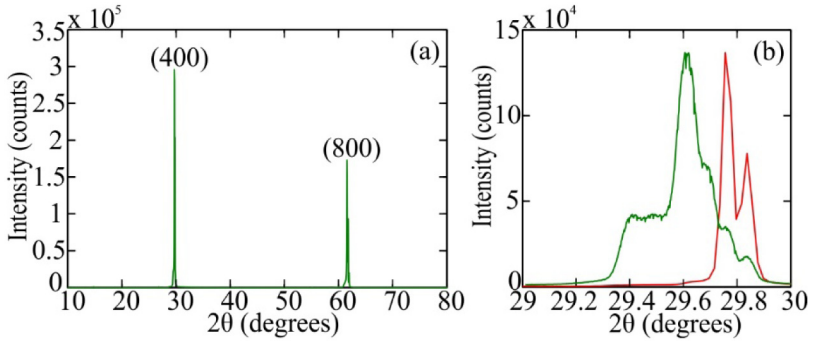

Fig. 2. XRD spectrum of (a) Yb(1.4%):YAG film, 2θ of 10° to 80°. (b) Yb(1.4%):YAG film (green) and blank YAG substrate (red), 2θ of 29° to 30°.

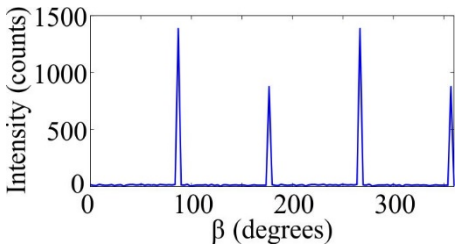

Fig. 3. XRD data of the Yb(1.4%):YAG film on <100> YAG displayed as an intensity profile at $\alpha = 0$ ° of a (400) pole figure with <100> orientation.

The aluminium deficiency in the deposited crystal layer manifests itself optically as an increase in the material's refractive index. To first order, there is a linear increase in the refractive index (r-squared of linear fit is 0.997, with a gradient of 0.146) with yttrium concentration, going from Al_2O_3 (1.755) through $Y_3Al_5O_{12}$ (1.815) to Y_2O_3 (1.902), at a wavelength of 1030 nm. From this we estimate the effect of a 2.5 at.% Al deficiency (and corresponding Y surplus) to produce an index increment of 3.65×10^{-3}. It is thus possible to tailor the numerical aperture of the waveguide through the stoichiometry of the material and, in our case, the aluminium deficiency in combination with the index increment from the incorporation of 1.4 at.% Yb [18], which leads to an estimated waveguide NA of ~0.1. An intensity profile at $\alpha = 0°$ of a (400) XRD pole figure with <100> orientation, is displayed in

#253375 Received 9 Nov 2015; accepted 30 Nov 2015; published 10 Dec 2015

Fig. 3. It shows 4 peaks with a separation of 90°, indicating that the film is a predominantly cubic highly-ordered crystal that follows the orientation of the substrate.

3.2. Spectroscopic characterization

For spectroscopic analysis the sample was excited by a diode laser operating at ~960 nm and the fluorescence from the PLD grown 1.4 at.% Yb:YAG film was captured using a multimode optical fiber connected to an optical spectrum analyzer (Ando AQ6317). For comparison a similar geometry comprising Czochralski-grown 10 at.% Yb:YAG crystal, was also measured using the same configuration and experimental conditions. The measured fluorescence lifetimes for both samples was ~950 μs. By applying the measured fluorescence lifetimes and Füchtbauer-Ladenburg equation [19], to the fluorescence spectrum, the emission cross sections for both samples are evaluated. Subsequently, the reciprocity method in combination with McCumber analysis is used to evaluate the absorption cross sections [20]. Since the emission peaks are at the same wavelengths for both the Czochralski- and PLD-grown samples, we have used literature values for the positions of the Stark levels within the $^2F_{7/2}$ and $^2F_{5/2}$ manifolds to evaluate the Boltzmann population factors [21]. Figure 4 presents absorption and emission cross sections from both samples. Spectroscopically, the most significant difference is in the emission cross section at 1030 nm, which has decreased by nearly 25%, but other changes include some smoothing of the low intensity peaks and a small increase in the bandwidth of the zero-phonon line from 2.6 nm (FWHM) for the Czochralski-grown crystal to 3.0 nm for the PLD-grown crystal. The reduction in the 1030 nm emission cross section is expected to increase laser thresholds for the PLD Yb:YAG in comparison to Czochralski-grown material.

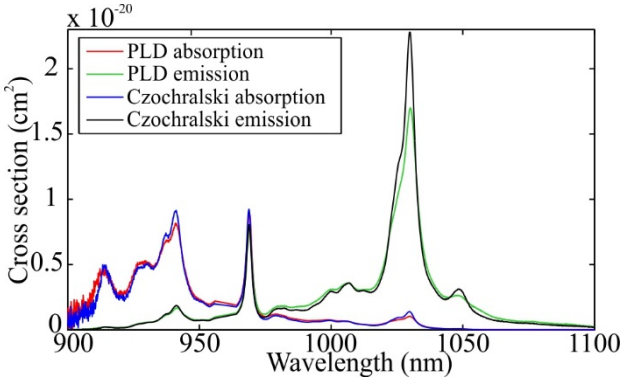

Fig. 4. Calculated absorption and emission cross sections from spectroscopic measurements of Czochralski- and PLD-grown Yb(1.4%):YAG.

4. Laser performance

To assess the suitability of the Yb(1.4%):YAG film for laser and amplifier applications the polished sample was built into a quasi-monolithic waveguide laser cavity, with the sample mounted on a water-cooled block to allow heatsinking. A pump in-coupling mirror (HT 950-990 nm, HR 1030-1100 nm) was placed in close proximity to the input facet. The pump beam (938 nm wavelength, 4 nm FWHM linewidth) was focused into the waveguide using a combination of cylindrical lenses producing a beam diameter (D4σ) of 10.6 μm in the guided (fast) axis by 1.5 mm in the unguided (slow) axis. The beam waist of the slow axis occurred at ~2.2 mm after that of the fast axis in air, corresponding to the longitudinal centre of the waveguide when the fast axis focus was arranged for optimal coupling. Due to the relatively low Yb dopant concentration of the film, a significant portion of the pump light passes through the guide without being absorbed. Our measurements of the transmitted pump agree well with calculations of a small-signal single-pass absorption of ~65% for the 8-mm-long

#253375 Received 9 Nov 2015; accepted 30 Nov 2015; published 10 Dec 2015

waveguide. Output power as a function of absorbed pump power for the waveguide laser with a 50% output coupler is displayed in Fig. 5. The collimated waveguide-laser output (1030 nm wavelength, 0.4 nm FWHM linewidth) was measured after reflection from a dichroic mirror (HT 900-990nm, HR1020-1100nm), and the absorbed pump power is calculated by subtracting the measured power of the light exiting the waveguide and transmitted through the same dichroic mirror from the incident pump power. The data point at 28.8 W abosprbed power is below the linear fit, indicating a possible onset of thermal roll-over. An insertion loss measurement for the waveguide was carried out with a HeNe and gave a propagation loss of less than 0.4 $dBcm^{-1}$.

A truncated image (due to the extreme aspect ratio of ~100:1) of the waveguide laser mode at the output mirror, taken using an Ophir-Spiricon SP620U beam profiling camera, is displayed in the inset to Fig. 5. As seen from the image, the spatial intensity distribution of the laser mode has no noticeable fine structure in the unguided direction, again implying the film is highly uniform with minimal defects. In contrast, in our previous work with Yb:Y_2O_3 films grown on <100> YAG we observed significant fine structure in the laser mode as a result of multiple domain growth and lattice mismatch between deposited layer and substrate [2]. This reaffirms our assessment that in this work with homo-epitaxial growth, the result of the deposition was a single-crystal film with a predominant (100) crystal orientation.

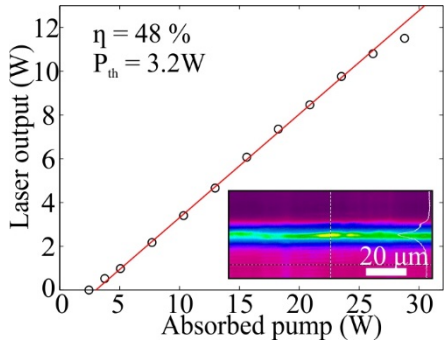

Fig. 5. Laser output performance as a function of pump power using a 50% output coupler. Inset: Image of the waveguide laser mode.

5. Conclusions

We have demonstrated the fabrication of a high-quality Yb(1.4%):YAG planar waveguide, grown via PLD. End-pumped with a diode-laser, a quasi-monolithic 11.5 W planar waveguide laser was realized, with 48% slope efficiency with respect to absorbed pump power. Analysis of the thin film shows excellent lattice matching, as would be expected with homo-epitaxial growth, and only one potential lattice orientation. Single-domain single-crystal growth was obtained with well-defined XRD peaks very close to accepted standard values. Due to the good lattice match between the undoped YAG substrate and Yb-doped deposited layer, minimal strain and associated defects were observed, suggesting even thicker films can potentially be produced without formation of cracks. Further improvement in the film quality is possible via tailoring of the final composition and homogeneity of the YAG layer through fine tuning of the deposition conditions. As such, it will be possible to engineer the dopant distribution and waveguide properties for bespoke active elements and improved power-scaling performance.

Acknowledgments

The authors acknowledge the support of the EPSRC through grant numbers EP/L021390/1, EP/N018281/1 and EP/J008052/1. The RDM data for this paper can be found at DOI: 10.5258/SOTON/383439

#253375 Received 9 Nov 2015; accepted 30 Nov 2015; published 10 Dec 2015